HHS Public Access

Author manuscript

Hepatology. Author manuscript; available in PMC 2019 November 01.

Published in final edited form as:

Hepatology. 2018 November ; 68(5): 1905–1921. doi:10.1002/hep.30061.

Interleukin 2 promotes hepatic regulatory T cell responses and protects from biliary fibrosis in murine sclerosing cholangitis

Amy E. Taylor[1], **Alexandra N. Carey**[1], **Ramesh Kudira**[1], **Celine S. Lages**[1], **Tiffany Shi**[1], **Simon Lam**[1,2], **Rebekah Karns**[1], **Julia Simmons**[1], **Kumar Shanmukhappa**[1], **Maha Almanan**[3], **Claire A. Chougnet**[3,4], and **Alexander G. Miethke**[*,1,4]

[1]Division of Pediatric Gastroenterology, Hepatology, and Nutrition, Cincinnati Children's Hospital Medical Center, Cincinnati, OH

[2]Department of Pediatrics, University of Calgary, Calgary, AB

[3]Division of Immunobiology, Cincinnati Children's Hospital Medical Center, Cincinnati, OH

[4]Department of Pediatrics, University of Cincinnati College of Medicine, Cincinnati, OH

Abstract

In the Mdr2−/− mouse model low phospholipid bile instigates biliary epithelial injury, sterile inflammation, and fibrosis, thereby recapitulating disease mechanisms implicated in biliary atresia (BA) and primary sclerosing cholangitis. We hypothesize that T-lymphocytes contribute to the biliary injury and fibrosis in murine sclerosing cholangitis (SC) and that they are susceptible to suppression by regulatory T cells (Tregs).

In juvenile Mdr2−/− mice, intrahepatic CD8 lymphocytes were expanded and contraction of intrahepatic Tregs coincided with rising serum alanine transferase (ALT) and alkaline phosphatase (ALP) levels between days 14-30 of life. Antibody-mediated depletion of intrahepatic CD8+ lymphocytes during that time reduced ALP levels and the expression of osteopontin (Opn), a pro-fibrogenic cytokine. Depletion of intrahepatic Tregs with anti-CD25 antibody between days 7-30 increased intrahepatic CD8+ T cells, Opn-expression and fibrosis. Conversely, expansion of intrahepatic Tregs with interleukin 2/anti-interleukin 2 immune complexes (IL-2c) downregulated hepatic expression of Opn and Tnfα, reduced frequency of intrahepatic CD8+ lymphocytes, and diminished biliary injury and fibrosis. Treatment with IL-2c upregulated hepatic Treg expression of CD39, an ectonucleotidase capable of hydrolyzing pro-inflammatory ATP. *In vitro*, Tregs expressing CD39 suppressed the proliferation of hepatic CD8+ lymphocytes from Mdr2−/− mice more efficiently than those lacking CD39. In infants with BA, infiltration of interlobular bile ducts with CD8+ cells was associated with biliary expression of OPN and its transcription was negatively correlated with mRNA expression of Treg-associated genes.

Conclusion—Hepatic CD8+ T lymphocytes drive biliary injury and fibrosis in murine SC. Their proliferation is controlled by hepatic Tregs via the purinergic pathway which are responsive to IL-2c, suggesting that Treg-directed low-dose Il-2 treatment may be considered as novel therapy for SC.

[*]**Corresponding author**: Alexander G Miethke, MD, Mail location 2010, 3333 Burnet Avenue, Cincinnati, Ohio, 45229-3026, Tel: 1-513-636-9078, Fax: 1-513-636-7805; Alexander.Miethke@cchmc.org.

Keywords

Primary Sclerosing Cholangitis; Regulatory T Cells; Purinergic Pathway; Biliary Atresia; osteopontin

Introduction

Fibrosing cholangiopathies including biliary atresia (BA) and primary sclerosing cholangitis (PSC) are characterized by inflammation and fibrosis centered on biliary epithelium with progressive cholestasis, bile duct proliferation, periductal sclerosis, and hepatic fibrosis resulting in end-stage liver disease which may require liver transplantation (1, 2). Adaptive immune responses are implicated in the pathogenesis of both conditions. In patients with BA, both the liver and bile duct remnants are infiltrated by inflammatory cells enriched in CD8+ lymphocytes (3). Furthermore, the presence of CD8+ T lymphocyte oligoclonal expansion suggests effector lymphocyte proliferation in response to a cognate antigen during the development of BA. In PSC, aberrant homing of gut-derived lymphocytes including CD8 T cells has long been described as a central component of immune-mediated bile duct injury (4). Yet, to what extent CD8 lymphocytes contribute to the progression of fibrosis in both conditions is largely undefined.

Regulatory T cells (Tregs), expressing the master regulatory transcription factor FOXP3, play an integral role in modulating inflammation and autoimmunity in disorders such as rheumatologic disease, graft-versus-host disease, inflammatory bowel disease, and liver allograft tolerance following transplantation. Treg dysfunction has in addition been linked to the effector immune response in the pathogenesis of BA, supported by reduced proportions of Tregs in peripheral blood at the time of diagnosis and increased lymphocyte reactivity to cytomegalovirus antigen (5). In patients with PSC, genome-wide association studies (GWAS) have identified gene polymorphisms encoding lymphocyte receptors on both effector cells and Tregs associated with an increased risk of PSC: the co-stimulatory receptor CD28 expressed on CD8+ effector lymphocytes and IL2RA (CD25) highly expressed on Tregs, respectively (6–8). The IL2RA polymorphism in patients with PSC was associated with decreased Treg number and suppressive function (8). Furthermore, a recent meta-analysis of published genome-wide association and liver transcriptomic studies revealed common disease pathways and central roles for FOXP3, STAT3, IL6, and TNFα in the three most common cholangiopathies PSC, BA and PBC (9).

Of note, predisposition to pediatric autoimmune liver disease has recently been linked to dysfunction of Tregs expressing CD39 (10). CD39 is a member of the ectonucleoside triphosphate diphosphohydrolase (E-NTPDase) family, which have been shown to hydrolyze pro-inflammatory ATP to ADP and finally adenosine which inhibits cytotoxic lymphocyte activation and reduces production of pro-inflammatory cytokine upon activation of the adenosine A2A receptor (11, 12). CD39 stabilizes the suppressor phenotype of Tregs under inflammatory conditions, and enhances their suppressor activity (13). There is emerging evidence that CD39+ CD4+ cells prevent ischemia reperfusion inflammatory liver injury,

promote liver allograft tolerance in mice, and have profound effects on anti-tumor immune surveillance in the liver (14–17).

The Mdr2 (Abcb4) knockout mouse is an established preclinical model of fibrosing cholangiopathy whereby absence of the phospholipid floppase Mdr2 at the hepatocyte canalicular membrane results in “toxic” low phospholipid bile, precipitation of unopposed biliary bile acid and cholesterol, and subsequent sterile inflammation driving bile duct epithelial injury and rapidly progressive biliary fibrosis (18). The mice develop sclerosing cholangitis (SC) with cholestasis, bile duct proliferation, and bridging fibrosis (19, 20). In this model, there is altered expression and cellular localization of canalicular transporters early in the disease course, microcrystal formation in bile ducts, bile leak and disruption of basement membranes with subsequent sterile inflammation and neutrophil-recruitment to sites of injury (18, 21). Progression of biliary fibrosis in Mdr2−/− mice, which is established by 12 weeks of age and associated with portal hypertension, recapitulates progression of fibrosis in PSC and BA (19).

Although the contribution of adaptive immunity to disease initiation and progression of BA is well established in rotavirus-induced murine neonatal bile duct obstruction, the roles of CD8- and Tregs in sterile inflammation, specifically of hepatobiliary injury and fibrosis in Mdr2−/− mice are largely unknown (22, 23). We sought to further delineate the crosstalk between Tregs and effector lymphocytes in Mdr2−/− mice as a model of non-infectious rapidly progressive fibrosing cholangiopathy. We hypothesize that CD8+ T-lymphocytes are integral in the initiation of biliary epithelial injury and fibrosis in murine SC and are susceptible to control by CD39+ Tregs through modulation of the purinergic pathway of lymphocyte activation.

Experimental Procedures

HUMAN STUDIES

Hepatic microarray studies—Relative expression for *SSP1* and Treg-associated genes originated from hepatic microarray studies carried out on infants with EHBA at the time of diagnosis by intrahepatic cholangiograms (24). Detailed information on handling of liver biopsy samples, RNA labeling, chip hybridization, normalization procedures, and analysis of gene expression were deposited in Gene Expression Omnibus (GEO: GSE46995). In this study, cRNA pools were hybridized to oligonucleotide-based human HG-U133 Plus 2.0 Array (Affymetrix, Santa Clara, CA, USA) containing 54,681 probe sets. The study protocols conformed to the ethical guidelines of the 1975 Declaration of Helsinki and were approved by the human research committees of all participating institutions.

Immunofluorescence—Archived 4μm formalin fixed paraffin embedded (FFPE) liver sections from de-identified patients with BA were obtained from the BioBank at CCHMC. Sequential heat induced epitope retrieval (HIER), incubation with primary and with HRP-conjugated secondary antibodies, and tyramide signal amplification were performed using the PerkinElmer Tyramide Signal Amplification Kit (OP7TL2001KT; PerkinElmer), according to manufacturer recommendations. EDTA (pH=9) was used for antigen retrieval prior to incubation with antibodies against CD8 (clone SP57; Ventana Medical Systems,

neat) or cytokeratin (clone PAN-CK; ThermoFisher Scientific, 1:100 dilution), while citrate buffer (pH=6) was used before staining with antibodies against osteopontin (clone AF1433; R&D Systems Inc, 1:1000). Images were captured through automated tile scanning with an inverted Nikon Eclipse TiE widefield microscope (Nikon Instruments Inc, Tokyo, Japan) mounted with a fully motorized stage at 20x magnification with 1% overlap. Image analysis was performed on tiled images using Nikon Elements Advanced Research.

MURINE STUDIES

Mice in a BALB/c background with Mdr2 deletion, a generous gift from Professor Lammert (Homburg University; Homburg, Germany), were crossed with BALB/c mice transgenic for FoxP3-EGFP (Jackson Laboratory) in order to precisely track Tregs during SC progression. Mice were bred in-house and maintained in pathogen-free animal facilities with temperature-regulation and a 12-hour dark/light cycle. They were fed 5020 breeder chow with 9% fat (Cincinnati Lab Supply, Cincinnati, OH). To demonstrate the role of effector lymphocytes on hepatobiliary injury, male Mdr2−/− mice transgenic for FoxP3-GFP received intraperitoneal (i.p.) injections of antibody depleting CD8+ lymphocytes (100μg/dose; clone YTS169.4, BioXcell) or isotype control IgG2b (100μg/dose; clone LTF-2, BioXcell) twice weekly between day of life 15 and 30. Mice were given i.p. injections of anti-CD25 antibody (250μg/dose; clone PC-61.5.3, BioXcell) or isotype control IgG1 (250μg/dose; HPRN, BioXcell) twice weekly between day of life 7 and 30 for Treg depletion. Mdr2−/− and +/- mice transgenic for FoxP3-GFP were subjected to i.p. administration of recombinant murine interleukin (IL)-2 (0.01μg/g; Catalog # 212-12, PeproTech) complexed to anti-IL2 (0.05 μg/g; clone Jes6-1A12, BioXCell) or PBS control twice weekly from day of life 8 until 30. The animal care and use committee of the Cincinnati Children's Research Foundation (Cincinnati, OH) approved the protocols utilized in these studies.

Mononuclear Cell Isolation, Flow Cytometry, Gene Expression Studies, Protein Blot Analysis, Plasma Biochemistry and Cytokine Quantifications, Immunohistochemistry and Immunofluorescence—were performed as described by our group before (25–27). Details are available in Supplemental Data.

Histological Analysis—Blinded analysis using a validated, semi-quantitative scale from 1-4+ for bile duct proliferation was performed by pathologist K.S. on H& E stained liver sections. Masson's trichrome stained-liver sections were subjected to Aperio image analysis, as previously described (27, 28). Image analysis of Opn-, CK-19- and Sirius Red stained liver sections was performed by digital scanning of liver sections at 10x using a Nikon H550S (Nikon Instruments, Inc, Tokyo, Japan). Scanned slides were analyzed by fraction of DAB positive area or collagen staining in 15 randomly selected 1000um × 1000um sections per each liver sample using NIS-Elements software (Nikon Instruments, Inc, Tokyo, Japan).

Cell Culture Proliferation Assays—Splenic and hepatic CD8+ lymphocytes were isolated using beads (DynaBeads; ThermoFisher Scientific, Waltham, MA) and subjected to Cell Trace Violet staining at a concentration of 5μM (ThermoFisher Scientific, Waltham, MA) prior to culture assay. Bead isolation (Miltenyi Biotec, Cambridge, MA) of splenic

mononuclear cells yielded CD4+ cells and were further isolated into CD25+ or 25− cells using the kit. FACS (BD FACSARIA 1 and II; BD Biosciences, Franklin Lakes, NJ) was employed to separate Tregs based on expression of CD39. Cells at a concentration of 70,000/well were incubated in 96-well plates coated with 1μg/mL of anti-CD3e (clone 145-2C11, eBioscience) and 1μg/mL anti-CD28 (clone 37.51, eBioscience) for 3 days in medium containing RPM1 1640 with 10% FCS, 1% Penicillin/Streptomycin, 1% L-glutamine, and 100IU/mL human IL2.

Statistical Analysis—Differences of continuous variables between groups were assessed for statistical significance using the student t test with a p-value <0.05. Charts were generated using GraphPad Prism version 7 (GraphPad, La Jolla, CA). PROC GPLOT in SAS was used to generate spline curves fitting the observed numbers of liver infiltrating CD8- and Treg-lymphocytes between day 8 and 45 of life.

Results

Infiltration of the Liver by CD8+ T Lymphocytes Precedes Manifestations of the Sclerosing Cholangitis (SC) Phenotype in Juvenile Mdr2−/− Mice

To examine the temporal relationship between toxic bile-induced development of the SC phenotype and the kinetics of hepatic effector lymphocyte and Treg responses, we evaluated liver sections and biomarkers of hepatocellular and biliary injury as well as intrahepatic lymphocyte composition in Mdr2−/− mice transgenic for FoxP3-EGFP at defined time points between 8 and 45 days of life using FoxP3-EGFP Mdr2+/- mice as controls. ALT and ALP levels were similar between both groups at days of life 8 and 14. Yet, ALT and ALP levels were significantly higher in Mdr2−/− compared to Mdr2+/- control mice beginning at day 30 (Fig 1A). Biochemical evidence of hepatobiliary injury in Mdr2−/− mice was temporally associated with histological evidence of SC, such as bile duct proliferation and periportal infiltration by immune cells (Fig 1B), and portal fibrosis (Fig 1C) at day 30. By day 45, the SC phenotype was fully developed with persistence of high ALT and ALP, increased bile duct proliferation, and portal-portal bridging of inflammatory infiltrates and fibrosis. Composition of liver infiltrating lymphocyte populations was determined at the 4 time points by flow cytometry and spline curves fitting the numbers of cells per time point were generated to delineate the kinetics of hepatic CD8- and Treg-responses in Mdr2−/− mice and in Mdr2+/- control mice without liver injury (Fig 1D). On average, numbers of intrahepatic CD8+ cells were higher in Mdr2−/− mice compared with age-matched Mdr2+/- mice at all time points and followed a cubic pattern with two inflection points in both genotypes (early trough at 15 days followed by temporary rise at 30 days). While emergence of hepatic Tregs followed a similar cubic pattern in Mdr2+/- mice, its kinetic appeared disrupted in Mdr2−/− mice with only a quadratic pattern (one inflection point). The Treg to CD8+ lymphocyte ratio is highest at day 15 in Mdr2−/− mice, but as their Tregs steadily decline in number after day 15 and CD8+ lymphocytes increase to day 30, the observed ratio at day 30 is the lowest, at which point liver injury becomes evident in Mdr2−/− mice. Temporal association between high Treg/CD8 ratios and lack of detectable liver injury at early time points raised the biological possibilities that CD8 cells contribute to liver injury in SC and that Tregs were capable of constraining CD8-mediated injury in this model.

Depletion of Effector Lymphocytes Diminishes Hepatobiliary Injury

In order to examine the role of CD8+ lymphocytes in the initiation of bile duct injury in juvenile Mdr2−/− mice, immunofluorescent staining was performed on liver sections from Mdr2−/− mice. It revealed localization of CD8+ lymphocytes in close proximity to bile duct epithelial cells (Fig 2A). Administration of antibodies depleting CD8+ lymphocytes between day 15 and 30 greatly reduced hepatic CD8+ lymphocytes (Fig 2B), decreased portal inflammation and diminished bile duct proliferation (Fig 2C), and correspondingly lowered serum ALP levels (Fig 2D). Osteopontin (Opn), a profibrogenic Th1 cytokine, has previously been linked to progression of fibrosis in human BA (29, 30). In Mdr2−/− mice, Opn expression was detected by immunohistochemistry in interlobular bile ducts, bile ductules, proliferating cholangiocytes, and zone 1 hepatocytes. We found that depletion of CD8+ lymphocytes reduced Opn expression by 64% (Fig 2E) indicating that CD8+ lymphocytes may instigate biliary fibrosis in Mdr2−/− mice via biliary epithelial injury.

Depletion of Hepatic Tregs Increases Hepatobiliary Injury and Fibrosis

Prompted by the observation that contraction of hepatic Tregs coincided with expansion of liver infiltrating CD8 lymphocytes and initiation of SC in Mdr2−/− mice, we further examined this relationship in Treg-depletion experiments. When anti-CD25 antibody was administered between days 7 and 30, the frequency of hepatic Foxp3+Tregs decreased by more than 80% (Fig 3A). While the frequency of total hepatic CD4+/CD3 cells not changed (data not shown), the frequency of hepatic CD8+ lymphocytes in αCD25-treated Mdr2−/− mice rose by 40%. Plasma levels for Tnfα increased by more than 2-fold compared with IgG-treated Mdr2−/− mice (Fig 3B). Depletion of Tregs not only resulted in more portal inflammation (Fig 3C) but also accelerated bile duct proliferation, as assessed by image analysis of CK19-stained bile duct profiles (Fig 3D), serving as surrogate histopathological marker for biliary injury in SC. Treatment of Mdr2−/− mice with αCD25 antibodies induced expression of Opn in BECs and periportal stromal cells (Fig 3E), which was associated with increased hepatic fibrosis, as assessed by image-analysis of Sirius Red stained liver sections (Fig 3F).

Cytokine-Induced Expansion of Hepatic Tregs Suppressed Hepatic Effector CD8+ Lymphocyte Responses

Next, we adopted a complementary approach and expanded Tregs in Mdr2−/− mice by administrating IL-2c between days 8 and 30. IL-2c has previously been shown to expand Tregs while blocking IL-2 agonistic effects on CD8+ and NK lymphocyte populations (31). Treatment with IL-2c significantly increased the frequency of Tregs/CD3+ lymphocytes by more than 100% in Mdr2+/- mice and by 50% in Mdr2−/− compared with PBS-treated age-, gender- and genotype-matched control animals (Fig 4A). Augmentation of the Tregs was accompanied by significant reduction of hepatic CD8+ lymphocytes in Mdr2−/− mice (but not in non-cholestatic Mdr2+/- mice) and an increase in Treg/CD8+ ratio by more than 2-fold. IL-2c treatment did not affect the proportions of hepatic NK cells (data not shown). Flow-cytometric findings were corroborated by down-regulation of mRNA expression for the *CD8a* gene. (Fig 4B). Furthermore, hepatic expression of genes implicated in T cell polarization (*Stat4*) and inflammation (*Nfkb1, Il1a*) were reduced in Mdr2−/− mice treated

with IL-2c as revealed by multiplex gene expression studies. Candidate gene qPCR studies showed significant down-regulation of hepatic expression for *Spp1* (encoding Opn) and *Tnfa* in IL-2c treated Mdr2−/− mice (Fig 4C). Immunoblotting on corresponding liver samples demonstrated reduced hepatic Tnfα protein expression in IL-2c treated Mdr2−/− mice (Fig 4D).

Expansion of Tregs Reduces Cholestasis, Biliary Injury, and Fibrosis

To evaluate whether cytokine-induced expansion of hepatic Tregs modulates the SC phenotype in Mdr2−/− mice, liver histopathology was assessed on H&E stained liver sections using a validated 1-4+ scale. Blinded review showed lower scores for bile duct proliferation in IL-2c-treated Mdr2−/− mice (Fig 5A/B). Reduced biliary injury was corroborated by results of image analysis of percent area of CK19+ cells (Fig 5C) and by significantly lower ALP levels in IL-2c-treated Mdr2−/− mice (Fig 5D). Decreased biliary injury was accompanied by halted progression of fibrosis in IL-2c treated Mdr2−/− mice, as shown by down-regulation of mRNA-expression of the pro-fibrogenic gene smooth muscle actin (SMA; Fig 5E) and 50% reduction in fibrosis as determined by image analysis of trichrome-stained liver sections (Fig 5F).

Tregs Display an Activated Phenotype and Increased Ectonucleotidase Expression in Response to IL-2c In Vivo

To determine the effects of IL-2c on Tregs infiltrating the liver as the site of inflammation in Mdr2−/−, we determined the molecular phenotype of Tregs from livers and spleens of knockout and age-matched control mice using flow cytometry. Treatment with IL-2c significantly upregulated the activation marker ICOS on both hepatic and splenic Tregs in Mdr2−/− mice (Fig 6A). GITR, a corticosteroid-induced TNF receptor, is a costimulatory molecule expressed on T cells including Tregs (32). GITR was abundantly expressed on hepatic and splenic Tregs at baseline in Mdr2−/− mice (Fig 6B). Il-2c significantly upregulated GITR on liver infiltrating Tregs in non-cholestatic Mrd2+/- mice, but not in Mdr2−/− mice, indicating that the response of Tregs to IL-2c depends on the tissue microenvironment. High CD39 expression was restricted to Tregs in the liver (>40%) of untreated Mdr2−/− and +/- mice, as opposed to the spleen, and IL-2c treatment promoted a further surge of hepatic CD39+Tregs in Mdr2−/− mice (Fig 6C). Based on published data on the role of CD39+Tregs in inflammatory liver diseases, their higher frequency in the liver of Mdr2−/− mice compared with secondary lymphoid organs (spleen), and their response to Il-2c treatment, we hypothesized that CD39 was important in mediating Treg-suppression of CD8 lymphocytes in SC.

CD39+ Tregs Efficiently Suppress Proliferation of Hepatic CD8 Lymphocytes from Mdr2−/− Mice

Co-culture experiments were performed to determine the direct effect of Tregs on CD8 proliferation. *In vitro*, isolated splenic CD8+ cells proliferated better with the addition of non-Treg CD25-CD4+ lymphocytes, as demonstrated by reduction of the percentage of non-proliferating CD8 lymphocytes from 50.6 to 14.2%. Co-culture with CD4+CD25+ Tregs failed to boost proliferation (Fig 7A). In order to examine whether the purinergic pathway is involved in the control of CD8 lymphocyte activation and proliferation in SC, we determined

expression of the adenosine A_2A receptor, a G_S-protein which leads to intracellular accumulation of cAMP promoting inhibitory cellular responses, on CD8 lymphocytes and found that hepatic CD8 cells from Mdr2−/− mice upregulated A_2A receptor when co-cultured with Tregs (Fig 7B). Next, we investigated whether the CD39-A_2A receptor immunoregulatory circuit is relevant in control of CD8 proliferation in SC. Tregs from IL-2c treated Foxp3 EGFP mice were separated into CD39+ and CD39- populations by FACS and subsequently co-cultured with hepatic CD8 lymphocytes from Mdr2−/− mice. (Fig 7C). Only CD39+ Tregs, but not CD39- Tregs, inhibited proliferation of hepatic CD8+ lymphocytes from Mdr2−/− mice compared with co-culture with non-Treg CD4+ cells (Fig 7D). Our in vitro data demonstrates an important role for inhibition of hepatic CD8 lymphocyte responses in Mdr2−/− mice which is restricted to CD39+Tregs capable of direct suppression of proliferation which involves hydrolysis of pro-inflammatory ATP and suppressor effects of adenosine on A_2A receptor+CD8+ lymphocytes. Immunotherapy with IL-2c expands this potent subset of CD39+Tregs in the liver of Mdr2−/− mice.

Biliary Infiltration with CD8+ Lymphocytes is Associated with OPN Expression in Infants with BA at Diagnosis

FFPE liver sections from eight patients with BA at diagnosis (5 males, mean age 55 days) were subjected to multi-parameter IF against PAN-CK, CD8 and OPN and subsequent image analysis. The mean area of liver tissue imaged was 86.2 ± 14.3mm^2 per patient. CD8+ cells accumulated in the portal tracts (Fig 8A). CD8 cells infiltrating biliary epithelium (iCD8) were identified by CD8 cells overlapping with areas of cytokeratin and the degree of CD8 infiltration varied between portal tracts and patients (Fig 8B/C). Similar to our results in the murine model, OPN was primarily localized to interlobular bile ducts, bile ductules and proliferating cholangiocytes, with relatively minor expression in hepatocytes. Bile ducts with high grade of CD8 infiltration expressed more OPN than cholangiocytes without iCD8 (Fig B/C). Using image analysis, we found significant correlation between expression of OPN by cholangiocytes and number of iCD8 cells (Fig 8D). In order to test for an association between expression of *SPP1* and Tregs we surveyed previously performed microarray-based gene expression data on 47 patients with BA at diagnosis (24). Applying a principle component analysis to a set of 700 probes of Treg-associated genes revealed that expression values for genes like *THBS1, HDAC2, HDAC4, HDAC7, HDAC9, DICER1, and RUNX1* were negatively correlated with expression of *SPP1* indicating that similar to our results in murine SC, Tregs may suppress hepatic OPN expression in infants with BA (Fig 8E).

Discussion

Here we report that waning intrahepatic Treg responses in juvenile Mdr2−/− mice coincide with expansion of intrahepatic CD8 lymphocytes and initiation of hepatocellular and bile duct epithelial injury and fibrosis. In vivo manipulation of Tregs in Mdr2−/− mice demonstrated an influence of hepatic Tregs on liver infiltrating CD8 cells, biliary injury, osteopontin expression and fibrosis. Direct control of CD8 proliferation by Tregs depends on modulation of purinergic pathways of effector lymphocyte activation via CD39. In infants with BA at diagnosis, infiltration of intrahepatic bile ducts with CD8 cells is associated with

aberrant expression of OPN, validating aspects of our findings in the experimental model of SC for human fibrosing cholangiopathies.

Experiments involving depletion of CD8 lymphocytes in juvenile Mdr2−/− mice highlight their role in SC; CD8-depleted animals display less biliary injury, as evidenced by reduced bile duct proliferation and lower serum ALP levels as biomarkers of cholangiocyte injury (33, 34). CD8+ T lymphocytes have been assigned pathogenic effector functions in a spectrum of immune-mediated liver diseases, including autoimmune hepatitis and PSC (35). A specific subset of CD8+ lymphocytes with absent expression of the regulatory molecule CD28 was enriched in livers of patients with PSC and secreted increased TNFα upon stimulation (7). CD8 lymphocyte injury was also found to be integral in the neonatal bile duct injury of BA (5, 36). Previous studies have focused on the roles of CD8+ lymphocytes following viral infection affecting the biliary tree or in adoptive transfer models using immunocompromised mice and antigen-specific T-lymphocytes to generate cholangitis (22, 37). Our studies provide evidence that CD8+ lymphocytes are also important for initiation of cholangiocyte injury and fibrosis in the Mdr2−/− murine model of SC, which lacks an infectious insult or genetic predisposition to immune-mediated injury.

CD8+ lymphocyte depletion reduces expression of OPN, a pro-fibrogenic cytokine and driver of bridging fibrosis, suggesting that effector CD8+ cells perpetuate biliary fibrosis via induction of OPN expression in murine SC. Recent studies have demonstrated OPN to be a cytokine with pleiotropic effects on cell proliferation, migration, inflammation, and fibrosis (38–40). In experimental models of cholestasis, Opn has been linked to hepatic fibrosis via modulation of TGF-β and subsequent interaction with hepatic stellate cells and their transformation into collagen-1 secreting myofibroblasts (40). In human disease, OPN expression is correlated with the stage of biliary fibrosis in infants with BA (30). Based on our findings in the Mdr2−/− mouse and in liver samples from infants with BA, we propose that CD8 lymphocytes are activated early in the pathogenesis of SC, contribute to the bile duct epithelial injury, and via induction of OPN in biliary and stromal cells to initiation of biliary fibrosis.

Importantly, we found that both CD8 responses and the SC phenotype are controlled by Tregs in Mdr2−/− mice. Depletion of Tregs with anti-CD25 antibodies promotes infiltration of the liver with CD8 lymphocytes, raises levels of circulating Tnfα, aggravates bile duct proliferation, induces Opn expression by biliary epithelial and periportal stromal cells and ultimately enhances fibrosis. In contrast, IL-2c mediated expansion of Tregs diminishes hepatic CD8 responses, down-regulates pro-inflammatory and Th1 cytokine production in the liver (Opn and Tnfα), and attenuates the SC phenotype. The latter results lend functional significance to GWAS which identified risk alleles in IL-2 and IL2RA in patients with PSC (6, 41), suggesting that alterations in the IL-2 pathway and subsequent effects on Treg homeostasis may represent important susceptibility factors for disease pathogenesis. Here we show in Mdr2−/− mice recapitulating the biliary fibrosis observed in PSC, that hepatic Treg homeostasis depends on IL-2, and that low-dose IL-2 treatment is able to overcome Treg deficits by increasing their number and activation status as evidenced by upregulation of ICOS and CD39 with beneficial effects for the liver disease phenotype including bile duct proliferation and fibrosis. However, compared with non-cholestastic Mdr2+/- mice, the

response of Mdr2−/− mice to treatment with IL-2c is attenuated indicating that cholestasis and/or the pro-inflammatory microenvironment in the liver of Mdr2−/− may partially block the mitogenic effects of IL-2 on Tregs. Future investigations need to reveal the mechanisms by which Treg homeostasis is altered under cholestatic conditions and how Treg-targeted immunotherapy can be optimized for these liver diseases. Resistance of Tregs to mitogens under certain conditions may explain that IL-2 treatment failed to protect Mdr2−/− mice from cholangitis in a recent study by a different group of investigators (42). This study was conducted in female C57BL6 Mdr2$^{-/-}$ as opposed to male BALB/c Mdr2−/− mice used in our study. Worse cholestasis in female versus male mice may have contributed to the resistance of Tregs (43). Effects of IL-2c treatment on expansion of CD39+ Tregs, CD8 lymphocyte responses, OPN induction and progression of biliary fibrosis was not investigated in that study.

Suppressive and anti-inflammatory ectonucleotidases such as CD39 have previously been suggested to provide a “molecular switch” to dampen tissue damage from liver inflammation (44). We report that CD8 lymphocytes from Mdr2−/− mice upregulate A_2A when co-cultured with CD4 lymphocytes and assign a critical role for CD39 in mediating Treg-suppressor function. Only Tregs expressing CD39 but not CD39- Tregs are capable of inhibiting the proliferation of hepatic CD8+ lymphocytes from Mdr2−/− mice in vitro. Furthermore, treatment with Il-2c not only increases the overall frequency of hepatic Tregs, but in particular the proportion of CD39+ Tregs in livers of Mdr2−/− mice, suggesting that the suppressive effects of IL-2 treatment on liver infiltrating CD8 lymphocytes and subsequent hepatobiliary injury in SC are mediated by CD39+ Tregs. This observation may be relevant for treatment considerations in PSC in which CD8 lymphocytes lack CD28 and are therefore resistant to Treg-control of dendritic-cell dependent co-stimulation (i.e. via CTLA-4), but may remain susceptible to direct inhibition by Tregs employing the CD39-A_2A immunoregulatory circuit.

We therefore conclude that in the Mdr2−/− model of fibrosing cholangiopathy with prominent sterile inflammation and rapid progression of fibrosis similar to those found in the majority of children with BA and in a subset of patients with PSC, CD8 lymphocytes contribute to bile duct epithelial injury and, via OPN expression, to fibrosis. These processes are susceptible to immunotherapy targeting Tregs, such as low dose IL-2, which boost intrahepatic Tregs, diminish CD8 responses, attenuate biliary injury and halt progression of fibrosis in this preclinical model. The purinergic suppressor pathway involving CD39 on Tregs and A_2A on CD8 cells is of particular importance in SC. Collectively, based on the results of our preclinical studies and of clinical trials in immune mediated liver disease, low dose IL-2 treatment should be considered as adjuvant therapy for fibrosing cholangiopathies like BA and PSC in the future (45, 46).

Supplementary Material

Refer to Web version on PubMed Central for supplementary material.

Acknowledgments

Financial Support:

Research supported by: NIH R01DK095001-05 (A.G.M), NIH T32DK007727-20 (PI: Lee Denson; support for A.E.T. and A.N.C.), the Browner Family Foundation, the Weidner Bea Strong Family Funding, the foundation "PSC Partners Seeking a Cure" (A.G.M), NIH P30DK0783 (Digestive Health Center), the American Association for Liver Diseases Foundation Advanced/Transplant Hepatology Fellow Award (A.E.T.), the National Institutes of Health Level VI Fellowship Award (A.N.C.), the American Liver Foundation Postdoctoral Research Fellowship Award (A.N.C.), the 2013 American Association for the Study of Liver Diseases Fellow Research Award (A.N.C.), and the University of Calgary Helios Scholarship (S.L).

List of Abbreviations

ALP	Alkaline Phosphatase
ALT	Alanine Transaminase
BA	Biliary Atresia
FFPE	Formalin fixed paraffin embedded
GWAS	Genome Wide Association Studies
HIER	Heat induced epitope retrieval
IL-2c	Interleukin 2/Anti-Interleukin 2 Immune Complexes
Opn/OPN	Osteopontin
PSC	Primary Sclerosing Cholangitis
SC	Sclerosing Cholangitis
Tregs	Regulatory T Cells

References

1. Asai A, Miethke A, Bezerra JA. Pathogenesis of biliary atresia: defining biology to understand clinical phenotypes. Nat Rev Gastroenterol Hepatol. 2015; 12:342–352. [PubMed: 26008129]
2. Karlsen TH, Folseraas T, Thorburn D, Vesterhus M. Primary sclerosing cholangitis - a comprehensive review. J Hepatol. 2017
3. Mack CL, Falta MT, Sullivan AK, Karrer F, Sokol RJ, Freed BM, Fontenot AP. Oligoclonal expansions of CD4+ and CD8+ T-cells in the target organ of patients with biliary atresia. Gastroenterology. 2007; 133:278–287. [PubMed: 17631149]
4. Grant AJ, Lalor PF, Salmi M, Jalkanen S, Adams DH. Homing of mucosal lymphocytes to the liver in the pathogenesis of hepatic complications of inflammatory bowel disease. Lancet. 2002; 359:150–157. [PubMed: 11809275]
5. Brindley SM, Lanham AM, Karrer FM, Tucker RM, Fontenot AP, Mack CL. Cytomegalovirus-specific T-cell reactivity in biliary atresia at the time of diagnosis is associated with deficits in regulatory T cells. Hepatology. 2012; 55:1130–1138. [PubMed: 22105891]
6. Webb GJ, Hirschfield GM. Using GWAS to identify genetic predisposition in hepatic autoimmunity. J Autoimmun. 2016; 66:25–39. [PubMed: 26347073]
7. Liaskou E, Jeffery LE, Trivedi PJ, Reynolds GM, Suresh S, Bruns T, Adams DH, et al. Loss of CD28 expression by liver-infiltrating T cells contributes to pathogenesis of primary sclerosing cholangitis. Gastroenterology. 2014; 147:221–232 e227. [PubMed: 24726754]
8. Sebode M, Peiseler M, Franke B, Schwinge D, Schoknecht T, Wortmann F, Quaas A, et al. Reduced FOXP3(+) regulatory T cells in patients with primary sclerosing cholangitis are associated with IL2RA gene polymorphisms. J Hepatol. 2014; 60:1010–1016. [PubMed: 24412607]

9. Luo Z, Jegga AG, Bezerra JA. Gene-disease associations identify a connectome with shared molecular pathways in human cholangiopathies. Hepatology. 2017
10. Grant CR, Liberal R, Holder BS, Cardone J, Ma Y, Robson SC, Mieli-Vergani G, et al. Dysfunctional CD39(POS) regulatory T cells and aberrant control of T-helper type 17 cells in autoimmune hepatitis. Hepatology. 2014; 59:1007–1015. [PubMed: 23787765]
11. Hausler SF, Montalban del Barrio I, Strohschein J, Chandran PA, Engel JB, Honig A, Ossadnik M, et al. Ectonucleotidases CD39 and CD73 on OvCA cells are potent adenosine-generating enzymes responsible for adenosine receptor 2A-dependent suppression of T cell function and NK cell cytotoxicity. Cancer Immunol Immunother. 2011; 60:1405–1418. [PubMed: 21638125]
12. Sitkovsky MV, Lukashev D, Apasov S, Kojima H, Koshiba M, Caldwell C, Ohta A, et al. Physiological control of immune response and inflammatory tissue damage by hypoxia-inducible factors and adenosine A2A receptors. Annu Rev Immunol. 2004; 22:657–682. [PubMed: 15032592]
13. Gu J, Ni X, Pan X, Lu H, Lu Y, Zhao J, Guo Zheng S, et al. Human CD39hi regulatory T cells present stronger stability and function under inflammatory conditions. Cell Mol Immunol. 2017; 14:521–528. [PubMed: 27374793]
14. Pommey S, Lu B, McRae J, Stagg J, Hill P, Salvaris E, Robson SC, et al. Liver grafts from CD39-overexpressing rodents are protected from ischemia reperfusion injury due to reduced numbers of resident CD4+ T cells. Hepatology. 2013; 57:1597–1606. [PubMed: 22829222]
15. Yoshida O, Dou L, Kimura S, Yokota S, Isse K, Robson SC, Geller DA, et al. CD39 deficiency in murine liver allografts promotes inflammatory injury and immune-mediated rejection. Transpl Immunol. 2015; 32:76–83. [PubMed: 25661084]
16. Cai XY, Ni XC, Yi Y, He HW, Wang JX, Fu YP, Sun J, et al. Overexpression of CD39 in hepatocellular carcinoma is an independent indicator of poor outcome after radical resection. Medicine (Baltimore). 2016; 95:e4989. [PubMed: 27749555]
17. Fu YP, Yi Y, Cai XY, Sun J, Ni XC, He HW, Wang JX, et al. Overexpression of interleukin-35 associates with hepatocellular carcinoma aggressiveness and recurrence after curative resection. Br J Cancer. 2016; 114:767–776. [PubMed: 27002937]
18. Fickert P, Fuchsbichler A, Wagner M, Zollner G, Kaser A, Tilg H, Krause R, et al. Regurgitation of bile acids from leaky bile ducts causes sclerosing cholangitis in Mdr2 (Abcb4) knockout mice. Gastroenterology. 2004; 127:261–274. [PubMed: 15236191]
19. Ikenaga N, Liu SB, Sverdlov DY, Yoshida S, Nasser I, Ke Q, Kang PM, et al. A new Mdr2(−/−) mouse model of sclerosing cholangitis with rapid fibrosis progression, early-onset portal hypertension, and liver cancer. Am J Pathol. 2015; 185:325–334. [PubMed: 25478810]
20. Popov Y, Patsenker E, Fickert P, Trauner M, Schuppan D. Mdr2 (Abcb4)−/− mice spontaneously develop severe biliary fibrosis via massive dysregulation of pro- and antifibrogenic genes. J Hepatol. 2005; 43:1045–1054. [PubMed: 16223543]
21. Cai SY, Mennone A, Soroka CJ, Boyer JL. Altered expression and function of canalicular transporters during early development of cholestatic liver injury in Abcb4-deficient mice. Am J Physiol Gastrointest Liver Physiol. 2014; 306:G670–676. [PubMed: 24481602]
22. Shivakumar P, Sabla G, Mohanty S, McNeal M, Ward R, Stringer K, Caldwell C, et al. Effector role of neonatal hepatic CD8+ lymphocytes in epithelial injury and autoimmunity in experimental biliary atresia. Gastroenterology. 2007; 133:268–277. [PubMed: 17631148]
23. Lages CS, Simmons J, Chougnet CA, Miethke AG. Regulatory T cells control the CD8 adaptive immune response at the time of ductal obstruction in experimental biliary atresia. Hepatology. 2012; 56:219–227. [PubMed: 22334397]
24. Moyer K, Kaimal V, Pacheco C, Mourya R, Xu H, Shivakumar P, Chakraborty R, et al. Staging of biliary atresia at diagnosis by molecular profiling of the liver. Genome Med. 2010; 2:33. [PubMed: 20465800]
25. Carey AN, Zhang W, Setchell KDR, Simmons JR, Shi T, Lages CS, Mullen M, et al. Hepatic MDR3 expression impacts lipid homeostasis and susceptibility to inflammatory bile duct obstruction in neonates. Pediatr Res. 2017; 82:122–132. [PubMed: 28355206]

26. Lages CS, Simmons J, Maddox A, Jones K, Karns R, Sheridan R, Shanmukhappa SK, et al. The dendritic cell-T helper 17-macrophage axis controls cholangiocyte injury and disease progression in murine and human biliary atresia. Hepatology. 2017; 65:174–188. [PubMed: 27641439]
27. Miethke AG, Zhang W, Simmons J, Taylor AE, Shi T, Shanmukhappa SK, Karns R, et al. Pharmacological inhibition of apical sodium-dependent bile acid transporter changes bile composition and blocks progression of sclerosing cholangitis in multidrug resistance 2 knockout mice. Hepatology. 2016; 63:512–523. [PubMed: 26172874]
28. He H, Mennone A, Boyer JL, Cai SY. Combination of retinoic acid and ursodeoxycholic acid attenuates liver injury in bile duct-ligated rats and human hepatic cells. Hepatology. 2011; 53:548–557. [PubMed: 21274875]
29. Whitington PF, Malladi P, Melin-Aldana H, Azzam R, Mack CL, Sahai A. Expression of osteopontin correlates with portal biliary proliferation and fibrosis in biliary atresia. Pediatr Res. 2005; 57:837–844. [PubMed: 15845635]
30. Huang L, Wei MF, Feng JX. Abnormal activation of OPN inflammation pathway in livers of children with biliary atresia and relationship to hepatic fibrosis. Eur J Pediatr Surg. 2008; 18:224–229. [PubMed: 18704890]
31. Boyman O, Kovar M, Rubinstein MP, Surh CD, Sprent J. Selective stimulation of T cell subsets with antibody-cytokine immune complexes. Science. 2006; 311:1924–1927. [PubMed: 16484453]
32. Ronchetti S, Zollo O, Bruscoli S, Agostini M, Bianchini R, N G, Ayroldi E, et al. GITR, a member of the TNF receptor superfamily, is costimulatory to mouse T lymphocyte subpopulations. Eur J Immunol. 2004; 34:613–622. [PubMed: 14991590]
33. de Vries EM, Wang J, Leeflang MM, Boonstra K, Weersma RK, Beuers UH, Geskus RB, et al. Alkaline phosphatase at diagnosis of primary sclerosing cholangitis and 1 year later: evaluation of prognostic value. Liver Int. 2016; 36:1867–1875. [PubMed: 26945698]
34. Krones E, Erwa W, Trauner M, Fickert P. Serum alkaline phosphatase levels accurately reflect cholestasis in mice. Hepatology. 2015; 62:981–983. [PubMed: 25424394]
35. Gravano DM, Hoyer KK. Promotion and prevention of autoimmune disease by CD8+ T cells. J Autoimmun. 2013; 45:68–79. [PubMed: 23871638]
36. Mack CL, Falta MT, Sullivan AK, Karrer F, Sokol RJ, Freed BM, Fontenot AP. Oligoclonal Expansion of CD4+ and CD8+ T-Cells in the Target Organ of Patients with Biliary Atresia. Gastroenterology. 2007; 133:278–287. [PubMed: 17631149]
37. Seidel D, Eickmeier I, Kuhl AA, Hamann A, Loddenkemper C, Schott E. CD8 T cells primed in the gut-associated lymphoid tissue induce immune-mediated cholangitis in mice. Hepatology. 2014; 59:601–611. [PubMed: 24038154]
38. Strazzabosco M, Fabris L, Albano E. Osteopontin: a new player in regulating hepatic ductular reaction and hepatic progenitor cell responses during chronic liver injury. Gut. 2014; 63:1693–1694. [PubMed: 25056656]
39. Coombes JD, Swiderska-Syn M, Dolle L, Reid D, Eksteen B, Claridge L, Briones-Orta MA, et al. Osteopontin neutralisation abrogates the liver progenitor cell response and fibrogenesis in mice. Gut. 2015; 64:1120–1131. [PubMed: 24902765]
40. Wang X, Lopategi A, Ge X, Lu Y, Kitamura N, Urtasun R, Leung TM, et al. Osteopontin induces ductular reaction contributing to liver fibrosis. Gut. 2014; 63:1805–1818. [PubMed: 24496779]
41. Liu JZ, Hov JR, Folseraas T, Ellinghaus E, Rushbrook SM, Doncheva NT, Andreassen OA, et al. Dense genotyping of immune-related disease regions identifies nine new risk loci for primary sclerosing cholangitis. Nat Genet. 2013; 45:670–675. [PubMed: 23603763]
42. Schwinge D, von Haxthausen F, Quaas A, Carambia A, Otto B, Glaser F, Hoh B, et al. Dysfunction of hepatic regulatory T cells in experimental sclerosing cholangitis is related to IL-12 signaling. J Hepatol. 2017; 66:798–805. [PubMed: 27965154]
43. Li X, Liu R, Yang J, Sun L, Zhang L, Jiang Z, Puri P, et al. The role of LncRNA H19 in gender disparity of cholestatic liver injury in Mdr2−/− mice. Hepatology. 2017
44. Vaughn BP, Robson SC, Longhi MS. Purinergic signaling in liver disease. Dig Dis. 2014; 32:516–524. [PubMed: 25034284]
45. Klatzmann D, Abbas AK. The promise of low-dose interleukin-2 therapy for autoimmune and inflammatory diseases. Nat Rev Immunol. 2015; 15:283–294. [PubMed: 25882245]

46. Koreth J, Matsuoka K, Kim HT, McDonough SM, Bindra B, Alyea EP 3rd, Armand P, et al. Interleukin-2 and regulatory T cells in graft-versus-host disease. N Engl J Med. 2011; 365:2055–2066. [PubMed: 22129252]

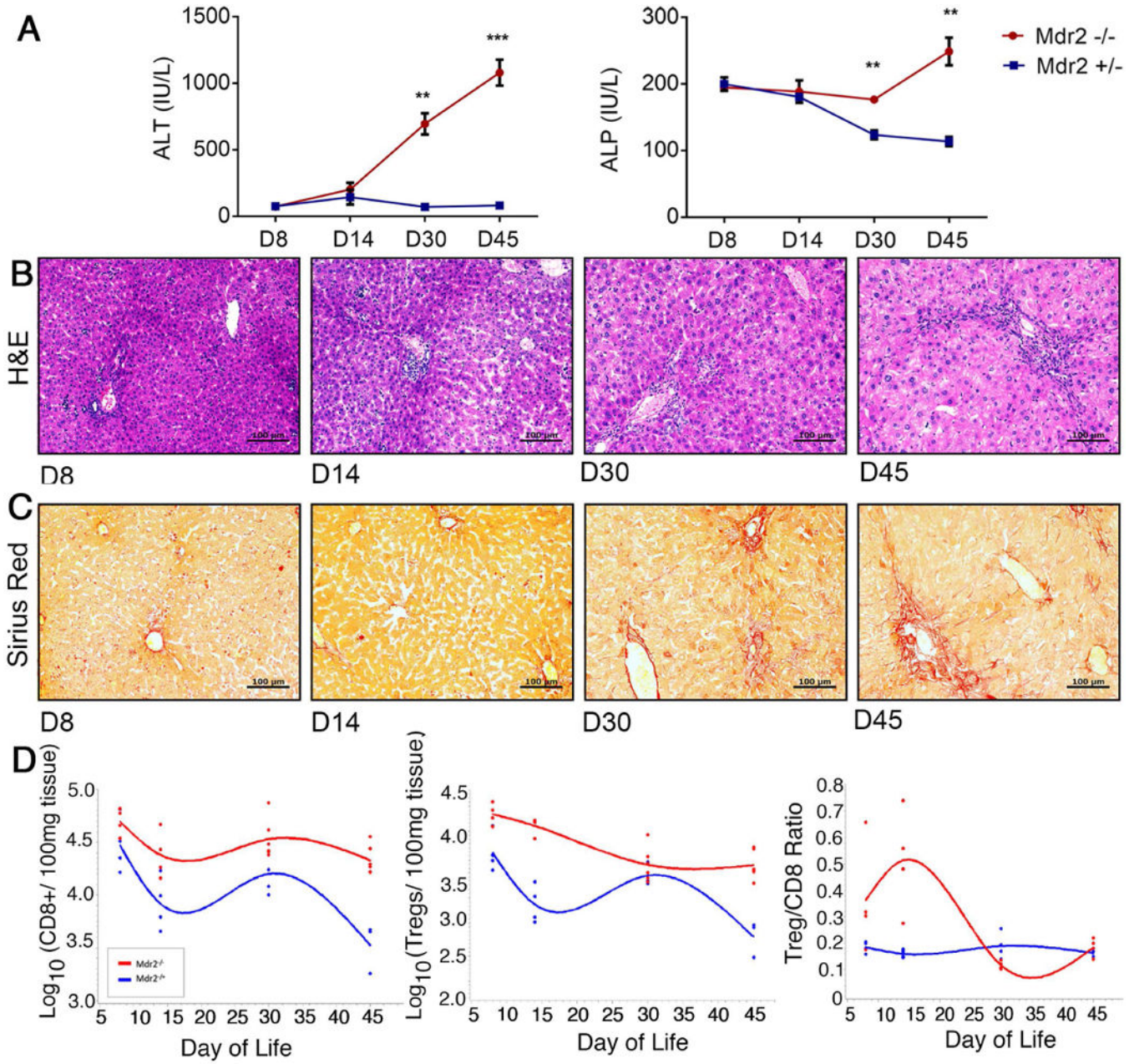

Fig. 1. Contraction of intrahepatic Treg lymphocytes coincides with hepatobiliary injury in Mdr2−/− mice

(A) Plasma ALT and serum ALP concentrations were measured in FoxpP3-EGFP Mdr2−/− and age-matched control Foxp3-EGFP Mdr2+/- mice between 8 and 45 days of life using colorimetric assays (n=3-4/per group). Differences between groups were tested for statistical significance using an unpaired t test with **p<0.01 and ***p<0.005. In **(B)** and **(C)**, representative photomicrographs of H&E and Sirius Red stained liver sections from Mdr2−/− mice demonstrate progression of periportal inflammation, bile duct proliferation and liver fibrosis. **(D)** Flow cytometry was performed on hepatic MNC from age-matched Mdr2−/− and +/- mice. Foxp3(GFP)+CD25+CD4+ Tregs and CD8+ T lymphocytes were enumerated

within CD3+ size-gated lymphocytes (n=4-6/group), and total numbers of cells were log-transformed. Spline curves were generated to describe the kinetics of numeric Treg and CD8 lymphocyte responses in the liver during the first 45 days of life.

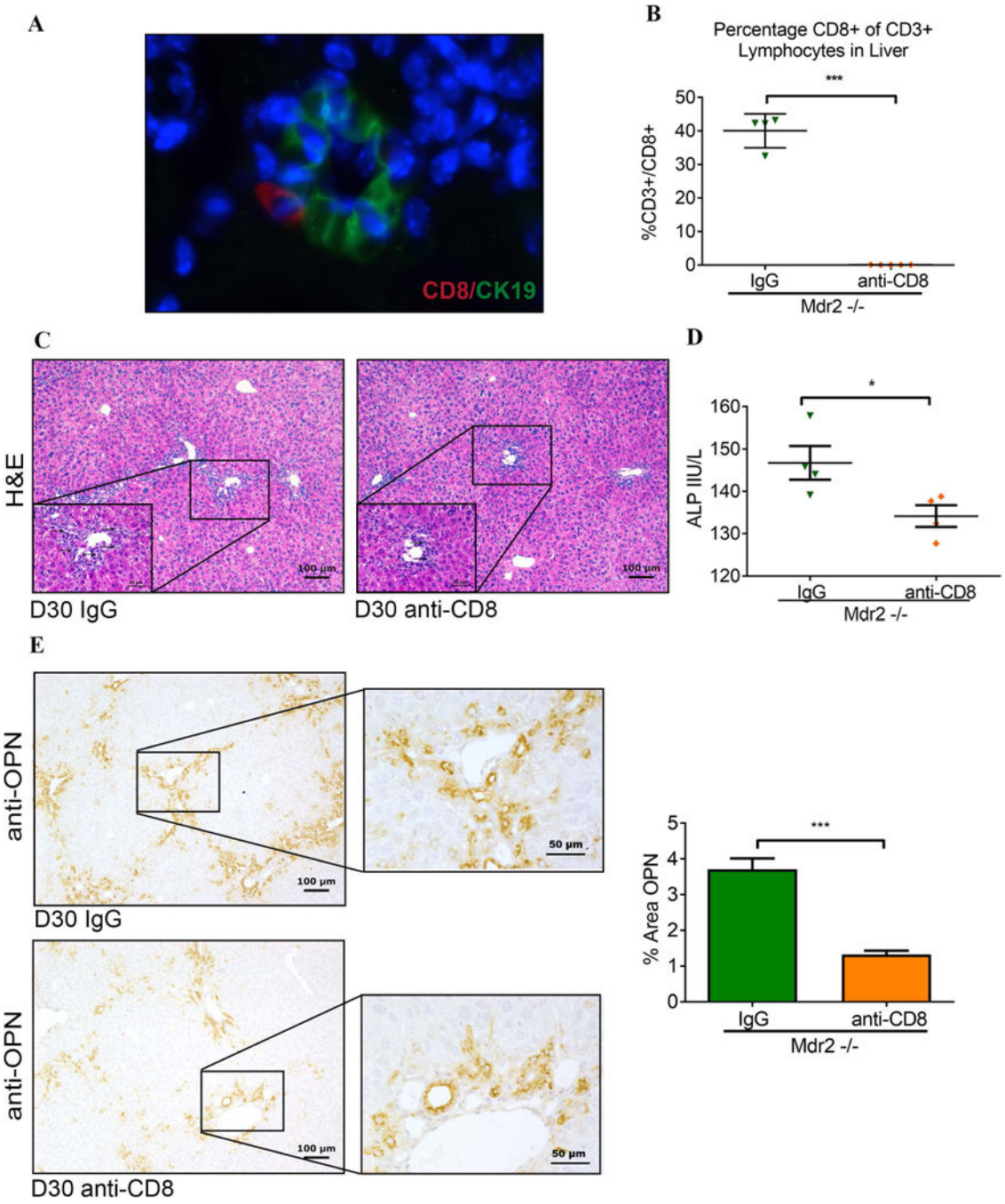

Fig. 2. Hepatic CD8+ T cells function as effector lymphocytes in "toxic bile" induced sclerosing cholangitis

(A) Liver sections from 30-day-old Mdr2−/− mice were subjected to dual immunofluorescence with antibodies against CD8 and CK19. CD8+ cells (red) were detected infiltrating interlobular bile ducts identified by immunoreactivity against the cholangiocyte marker CK19+ (green). **(B)** Male Mdr2−/− mice were injected i.p. with anti-CD8 antibody or IgG isotype control twice weekly between day of life 14 and 30 and hepatic MNC from 30-day-old mice were subjected to flow cytometry. **(C)** Representative

photomicrographs of H&E-stained liver sections demonstrate reduced bile duct proliferation in CD8-depleted Mdr2−/− mice (arrows denote bile duct profiles in high magnification inserts). **(D)** Serum ALP levels were measured on day 30 following anti-CD8 vs IgG treatment. **(E)** Liver sections from 30-day-old CD8-depleted and control Mdr2−/− mice underwent OPN immunohistochemistry as shown in representative photomicrographs. Immunoreactivity for OPN was quantified by automated image analysis (n=3 mice/group). Statistical analysis was performed by applying unpaired t test with *$p<0.05$ and ***$p<0.005$.

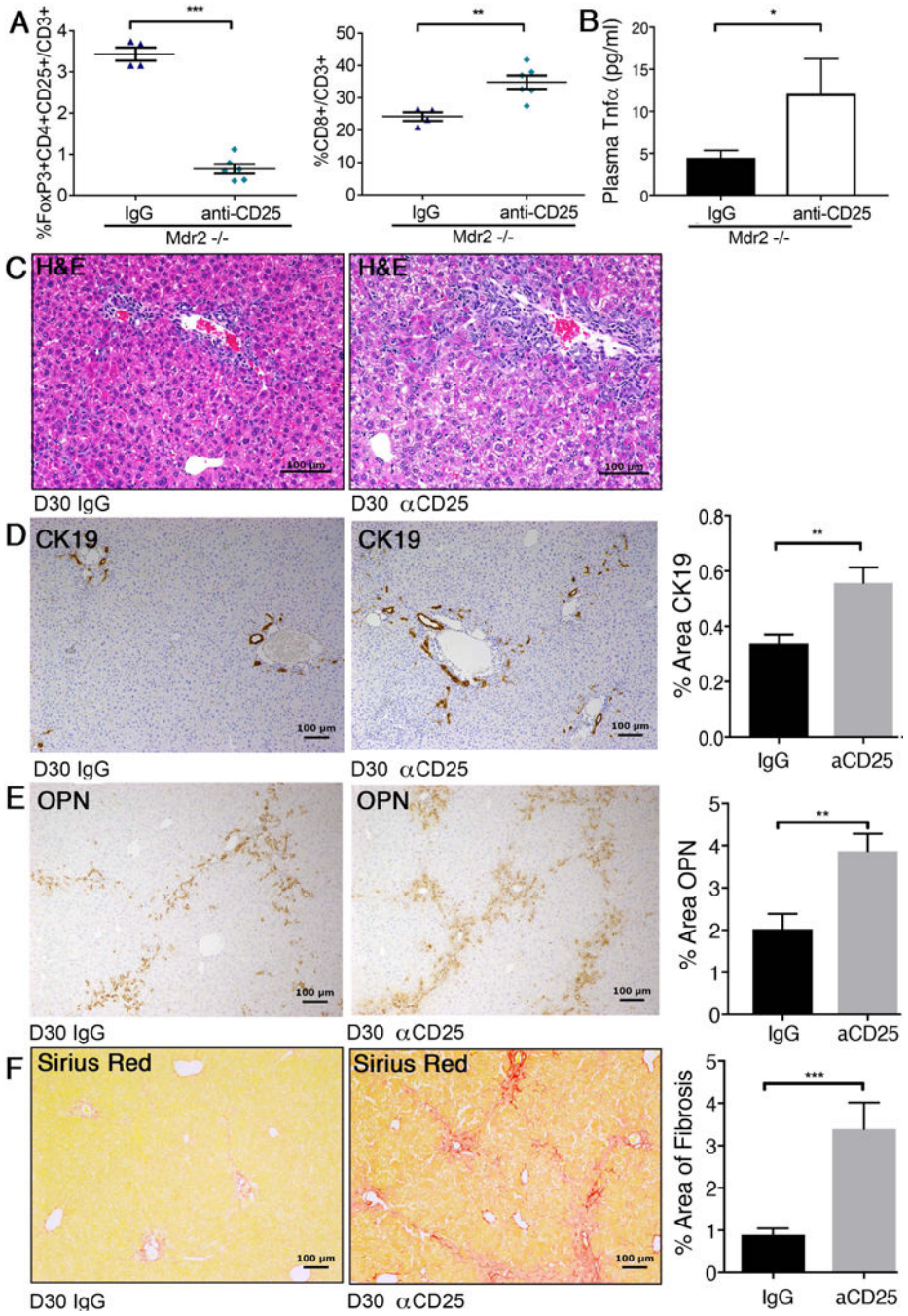

Fig. 3. Depletion of hepatic Tregs increases hepatic CD8+ lymphocytes, biliary injury, and fibrosis in Mdr2−/− mice

Juvenile Mdr2−/− mice transgenic for FoxP3-EGFP received i.p. injections of CD25-depleting antibody or IgG isotype control between day of life 7 and 30. Hepatic MNC from 30-day-old mice of both groups were subjected to flow cytometry to enumerate populations of FoxP3+CD25+ Treg and CD8+ lymphocytes **(A)**. Plasma concentrations for Tnfa were measured by Luminex **(B)**. Liver histology was assessed by H&E-stained liver sections from CD25-depleted and control 30-day-old Mdr2−/− mice and revealed increased periportal

inflammation in Treg-depleted mice as shown on representative photomicrographs **(C)**. Liver sections from both groups of mice were subjected to IHC against CK19 (**D**) and osteopontin (**E**), and to Sirius Red staining to evaluate fibrosis (**F**). Immunoreactivity and collagen deposition were quantified by image analysis. Differences between groups were tested for statistical significance using unpaired t test with *$p<0.05$, **$p<0.01$ and ***$p<0.005$.

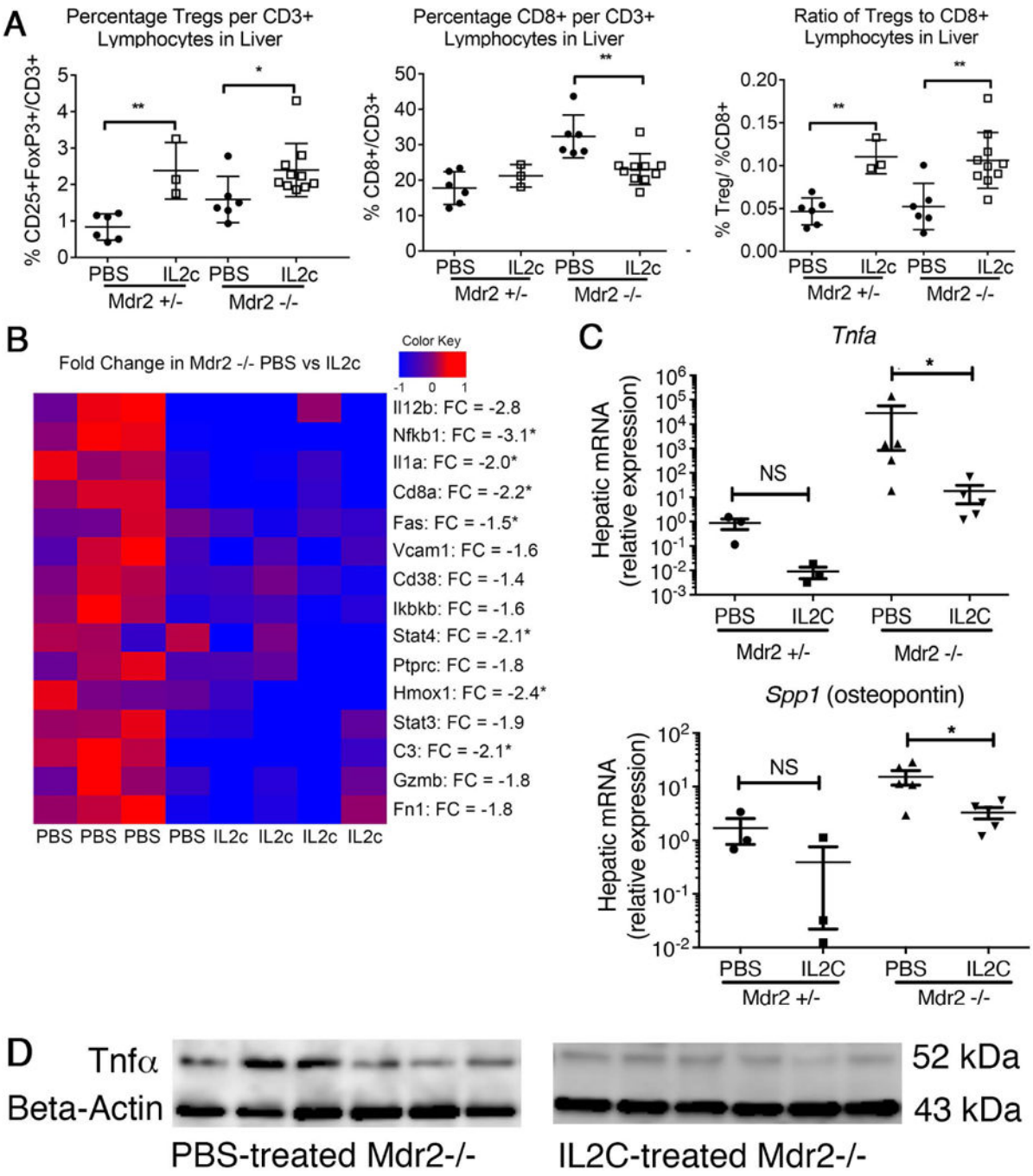

Fig. 4. IL-2c treatment augments hepatic Treg-responses and constrains liver inflammation

Male Mdr2−/− and age-matched heterozygous mice were treated with IL-2c (or PBS in controls) twice weekly from day of life 8-30. **(A)** Hepatic lymphocyte populations at day of life 30 were evaluated using flow cytometry and identified FoxP3(GFP)+CD25+CD4+ Tregs, CD8+CD3+ lymphocytes, and the ratio of Tregs to CD8+ lymphocytes. Quantitative RT-PCR using TaqMan multiplex arrays **(B)** or single probe assays **(C)** were performed on cDNA isolated from whole liver RNA to determine gene expression profiles. The heatmap was annotated with fold changes (FC) between average expression levels in the PBS- and

IL-2c-treated groups. Statistical significance was assessed with an unpaired t test with *p<0.05 and **p<0.01. **(D)** Tnfα protein concentration in corresponding liver samples was determined by western blotting.

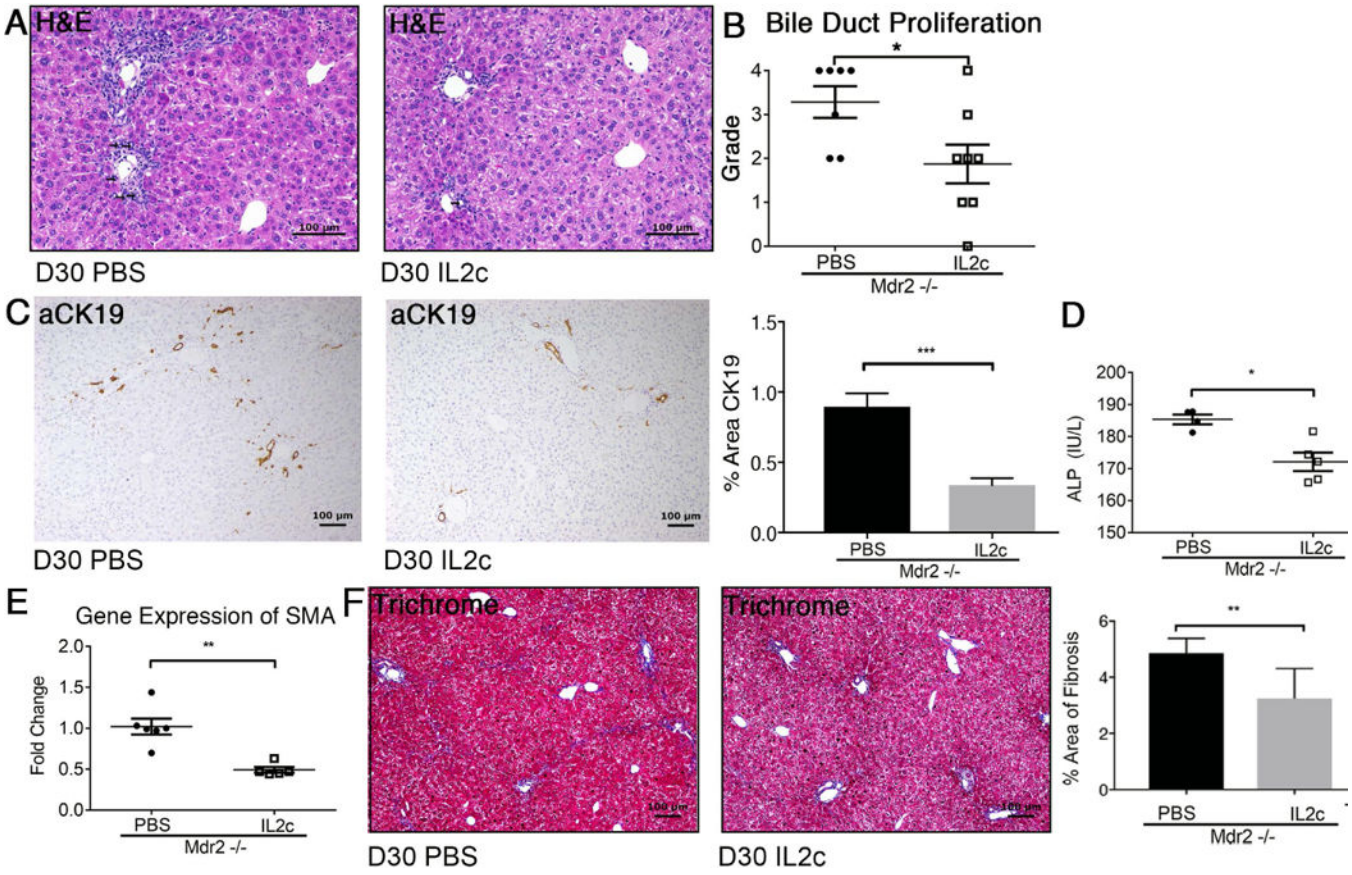

Fig. 5. IL-2c treatment attenuates biliary injury and liver fibrosis

Liver histopathology was assessed in 30-day-old male Mdr2−/− mice following treatment with IL-2c vs PBS between day 7 and 30. Arrows denote bile duct profiles on representative photomicrographs of H&E stained liver sections (**A**). Bile duct proliferation was graded by pathologists using a semi-quantitative scale from 1-4 **(B)**. Liver sections were subjected to anti-CK-19 immunohistochemistry and subsequent image analysis **(C)**. Serum ALP was measured in 30-day-old Mdr2−/− mice using a colorimetric assay **(D)**. Real-time PCR was performed for the pro-fibrogenic gene SMA from cDNA synthesized from whole liver RNA **(E)**. Trichrome-stained liver sections of Mdr2−/− mice treated with IL-2c verses PBS were analyzed utilizing Aperio Image Analysis to determine percent area of liver fibrosis **(F)**. Statistical significance was assessed with an unpaired t test with *p<0.05, **p<0.01, ***p<0.005.

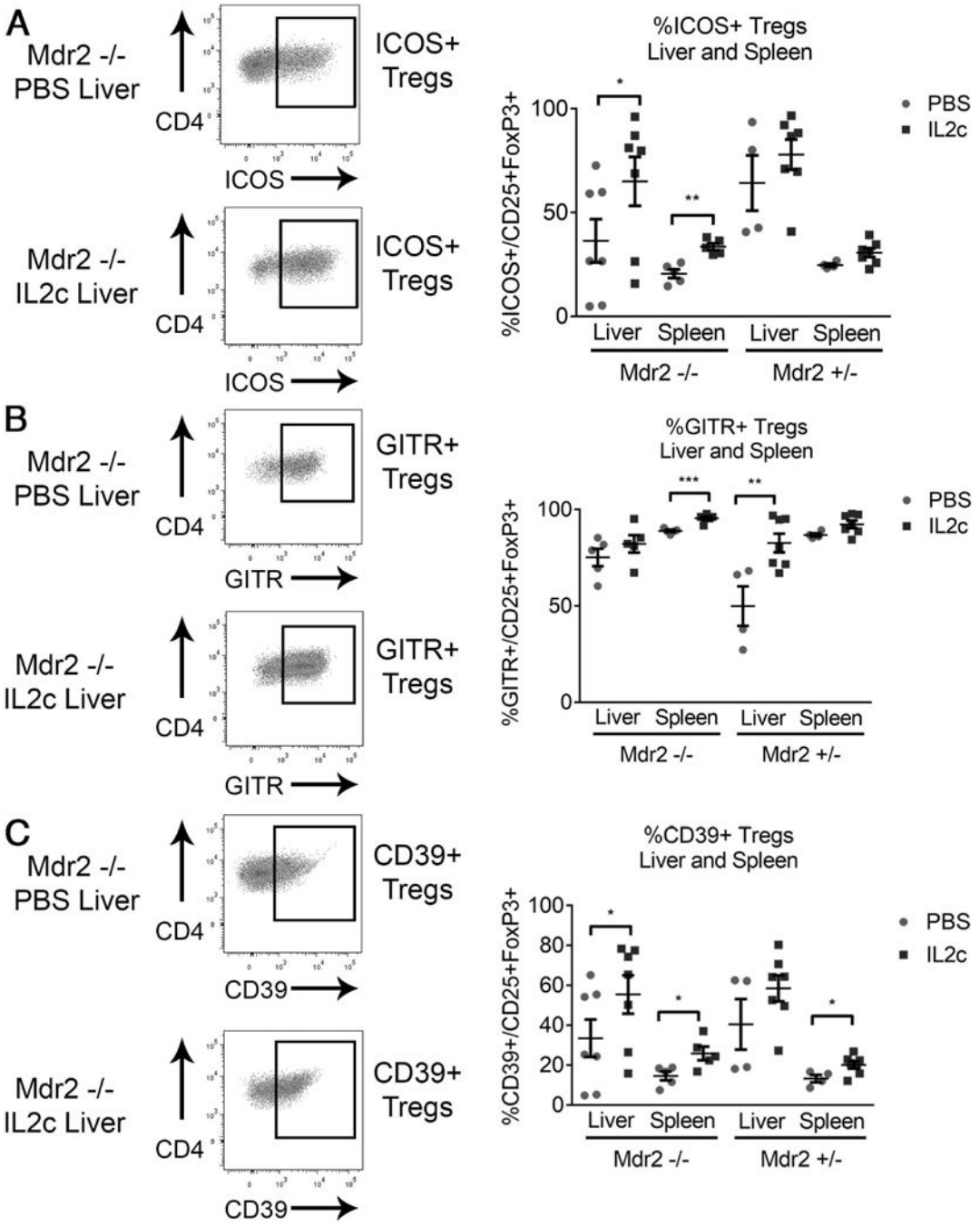

Fig. 6. Hepatic Tregs upregulate the activation markers ICOS and CD39 upon treatment with IL-2c

Male Mdr2−/− and age- and gender-matched heterozygous mice were treated with i.p. IL-2c (or PBS in controls) twice weekly from day of life 14-30. Flow cytometric analysis of hepatic and splenic mononuclear cells identified the proportion of CD3+CD4+CD25+FoxP3(GFP)+ Tregs displaying surface expression of the activation marker ICOS **(A)**, the suppressor molecule GITR **(B)**, and the ectonucleotidase CD39 **(C)**.

Statistical significance between two groups was assessed with an unpaired t test with *$p<0.05$, **$p<0.01$, and ***$p<0.005$.

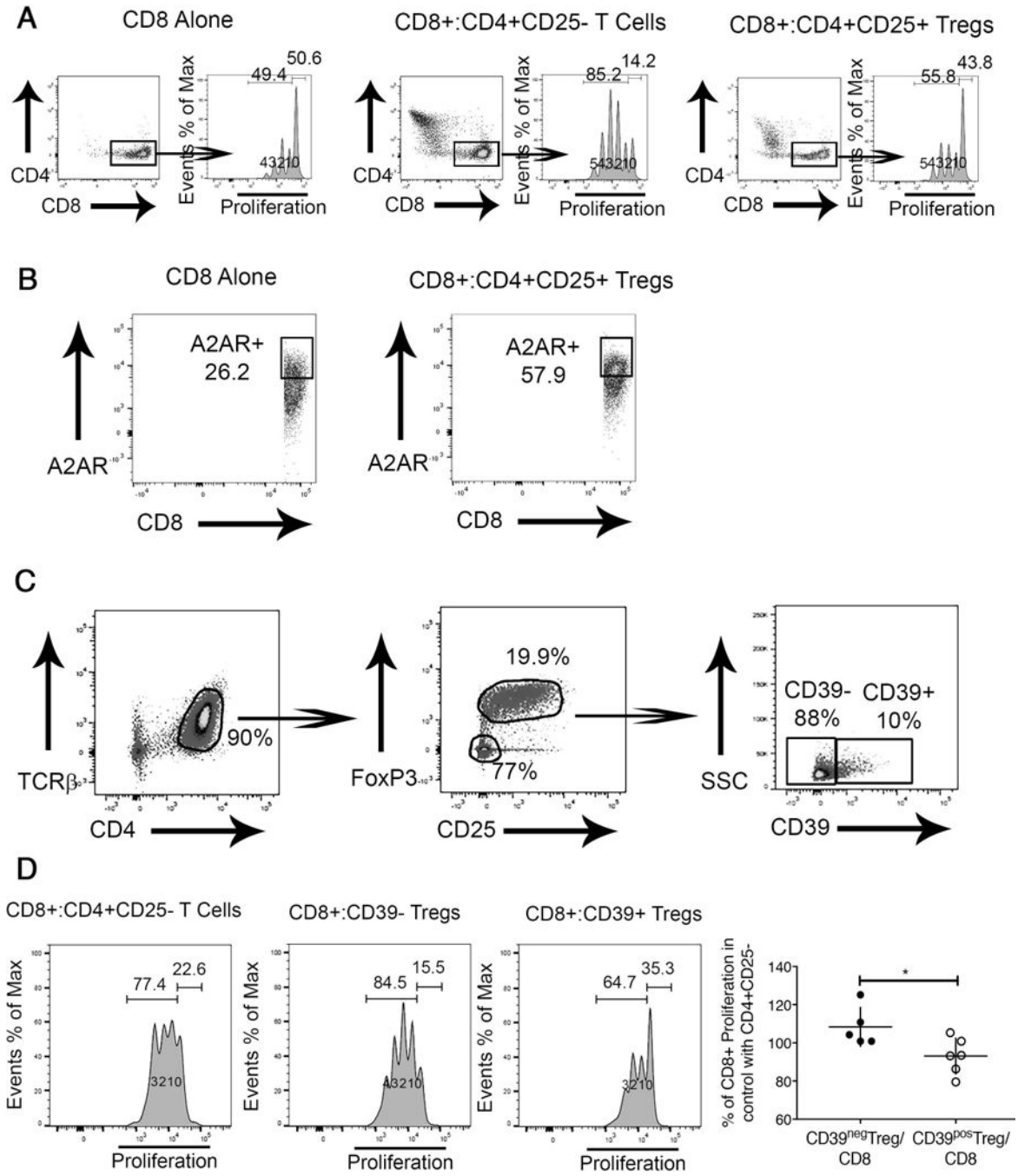

Fig. 7. Proliferation of hepatic CD8+ lymphocytes from Mdr2−/− mice is inhibited by Tregs in CD39-dependent manner

CD8+ lymphocytes were labeled with the proliferation tracker Cell Trace Violet and incubated in the presence of IL-2 and plate-bound anti-CD3, and anti-CD28. CD8+ lymphocyte proliferation was evaluated by flow cytometry based determination of Cell Trace Violet dilution after incubation for 3 days. Generation 0 defining non-proliferating and Generations 1-4 the proliferating cells in the CD8 compartment are denoted in the histograms. CD8+ cells were cultured alone or in the presence of splenic CD4+CD25- Non-Treg lymphocytes or CD4+CD25+ Tregs at a ratio of 1:1 **(A)**. Hepatic CD8+ cells from

Mdr2−/− mice were cultured alone or in the presence of splenic CD4+CD25+ Tregs at a ratio of 1:1 for 3 days with subsequent evaluation of the adenosine receptor A2A expression on CD8+ cells **(B)**. TCRβ+ CD4+ splenic lymphocytes were purified from adult Mdr2+/+ FoxP3-EGFP mice following treatment of i.p. IL-2c for 2 weeks and sorted by FACS into CD25-FoxP3- non-Tregs, CD39+, and CD39- Tregs **(C)** and co-cultured at a ratio of 1:1 with hepatic Cell Trace Violet labeled CD8+ T lymphocytes from adult Mdr2−/− mice for 3 days to determine percentage of proliferating CD8+ lymphocytes. CD8-proliferation in presence of CD39+ or CD39- Tregs was normalized against CD8-proliferation in co-cultures of CD8+ and non-Treg CD4+ cells assayed as internal standard in independent experiments. *$p<0.05$ in unpaired t test **(D)**.

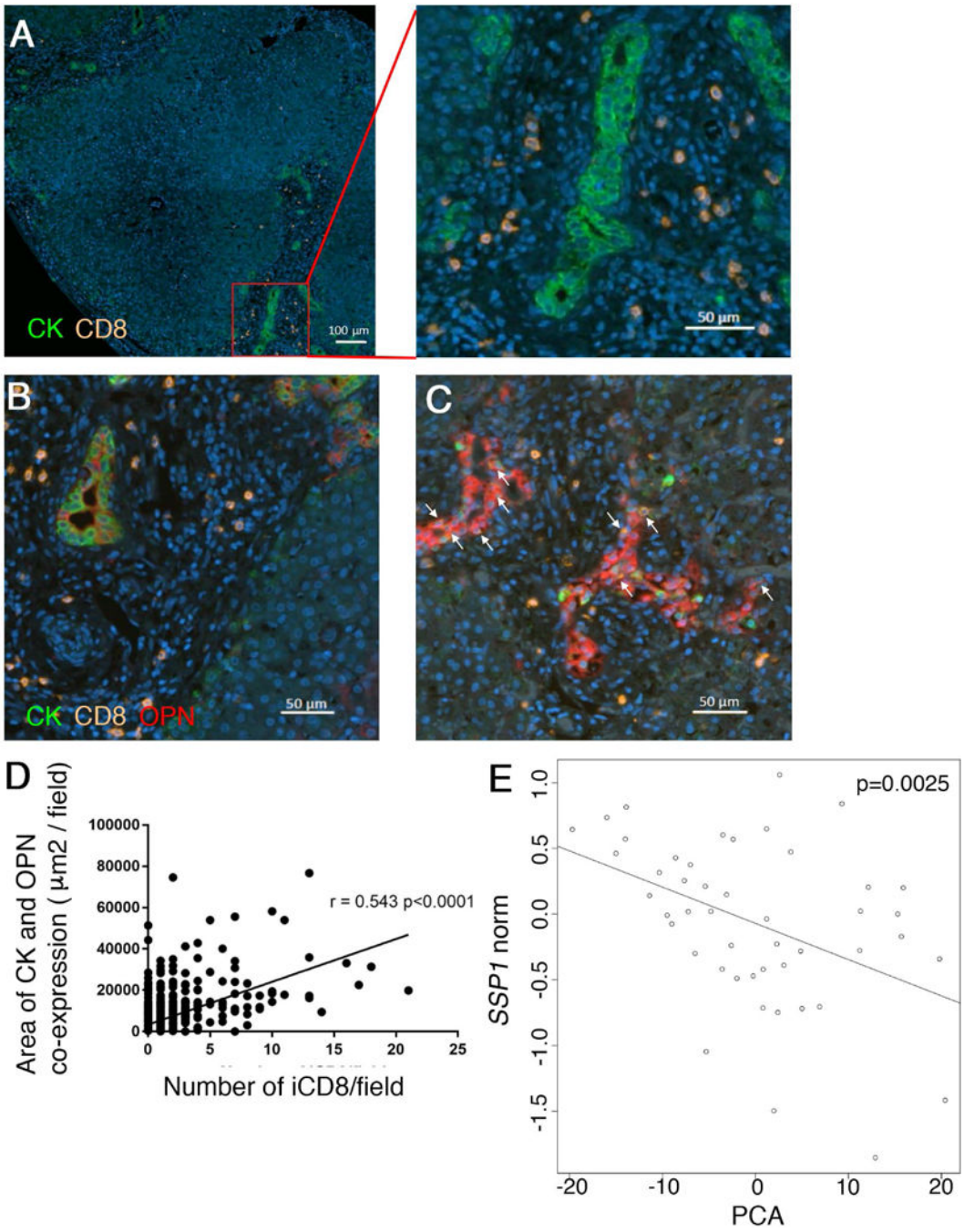

Fig. 8. Osteopontin expression by intrahepatic bile ducts is correlated with grade of infiltration by CD8 cells

Archived FFPE liver sections from 8 patients with BA at diagnosis were subjected to multi-parameter immunofluorescence with antibodies against Pan-CK, CD8 and oteopontin. CD8 cells accumulate in the periportal area in BA, as shown by representative photomicrographs **(A)**. CD8 cells infiltrating intrahepatic bile ducts (iCD8) are denoted by arrows and their number varies between patients and portal tracts. OPN expression by biliary epithelial cells is lower in samples without iCD8 (**B**) and up-regulated in presence of iCD8 (**C**). Co-

expression of Pan-CK and OPN was plotted against the number of iCD8 per filed, as determined by image analysis. The p-value represents the Pearson's correlation coefficient **(D)**. Microarray gene expression data from a cohort of 47 patients with BA at diagnosis was analyzed for expression values for *SSP1* (encoding OPN) and 120 Treg-associated genes. A negative correlation exists between *SSP1* expression and a principal component analysis of Treg-gene expression values as predictors **(E)**.